Characterization of the hydraulic performance of a gully under drainage conditions

Ricardo Martins, Jorge Leandro and Rita Fernandes de Carvalho

ABSTRACT

During rainfall events with low return periods (1–20 years) the drainage system can provide some degree of protection to urban areas. The system design is based not only on good hydraulic performance of the surface and the sewer network but also on their linking elements. Although the linking elements are of utmost importance as they allow the exchange of flow between the surface and the sewer network, there is a lack of studies that thoroughly characterize them. One crucial structural part of those elements is the gully. State-of-the-art dual-drainage models often use simplified formulae to replicate the gully hydraulic behaviour that lacks proper validation. This work focuses on simulating, both numerically and experimentally, the hydraulic performance of a 0.6 × 0.3 × 0.3 [m] (L × W × D) gully located inside an 8 × 0.5 × 0.5 [m] rectangular channel. The numerical simulations are conducted with the OpenFOAM toolbox and validated with water level measurements in the Multiple-Linking-Element experimental installation located at the Laboratory of Hydraulics of the University of Coimbra. The results provide a complete three-dimensional insight of the hydraulic behaviour of the flow inside the gully, and discharge coefficient formulae are disclosed that can be directly applied in dual-drainage models as internal boundary conditions.

Key words | computational fluid dynamics (CFD), gully, numerical modelling, OpenFOAM, urban drainage

Ricardo Martins (corresponding author)
Jorge Leandro
Rita Fernandes de Carvalho
Civil Engineering Department,
University of Coimbra,
Rua Luís Reis Santos,
3030-788 Coimbra,
Portugal
E-mail: *Ricardo.Martins@dec.uc.pt*

Jorge Leandro
Institute of Hydrology,
Water Management and Environmental Techniques,
IA 01/34, Ruhr-University Bochum,
44780 Bochum,
Germany

INTRODUCTION

During a rainfall event in urban areas the discharge waters are drained by two systems simultaneously, the surface (e.g., roads and channels) and the sub-surface (e.g., sewers and culverts) systems (Leandro 2008). While both one-dimensional (1D) and two-dimensional (2D) models have been used to model the surface system, for sub-surface modelling, 1D is the norm (Nasello & Tucciarelli 2005; Leandro *et al.* 2011). The 'dual-drainage' concept (Djordjević *et al.* 1999, 2005) is often used to model the surface and the sub-surface simultaneously (Chen *et al.* 2005, 2007). The linkage between these two systems can be undertaken through a conceptual model, e.g., the multiple-linking-element (Leandro *et al.* 2007) or through a mixture of weir and orifice equations (Chen *et al.* 2007). These equations can be either calibrated experimentally (Martins *et al.* 2010), or using computational fluid dynamics (CFD) simulations, usually three dimensions (3D) or 2D, that can simulate the complex hydraulics found in the linkage structure (Martins 2011; Carvalho *et al.* 2011).

A large contribution towards characterizing the efficiency of gullies (Storm Water Inlets) was made by Li and Geyer, who studied experimentally the flow through several types of gullies (Li *et al.* 1951a, b, 1954a, b; Bock *et al.* 1956).

Weir (1) or orifice (2) equations can be used with the coefficients obtained experimentally

$$Q_w = C_w * b_w * \sqrt{2 * g * H^3} \quad (1)$$

$$Q_o = C_o * A_o * \sqrt{2 * g * H} \quad (2)$$

where subscript '*w*' represents a weir variable and subscript '*o*' an orifice variable. Q represents the discharge, A the area of the orifice, b the width of the weir, g the acceleration (9.81 m/s^2), and H the uniform height of the discharge upstream of the weir/orifice.

This study aims to research the hydrodynamic behaviour of a gully under drainage conditions, and to develop coefficient discharge formulae that can be used as internal boundary conditions in dual-drainage models. The next

doi: 10.2166/wst.2014.168

section presents the methodology used to perform the experimental and numerical tests.

METHODOLOGY

Experimental facility and free surface detection

The experimental setup consists of a gully placed inside the wave channel at the hydraulics laboratory at the Department of Civil Engineering, University of Coimbra.

The channel is $8 \times 0.5 \times 0.5$ [m] (long × wide × height) with a gully with dimensions of $0.6 \times 0.3 \times 0.3$ [m]. At the bottom of the box, a circular hole with a 0.08 [m] diameter with an additional pipe of 0.05 [m] length with a free exit. The discharges tested are presented in Table 1. The discharge control was made using a SCADA system (Santos *et al*. 2008) that controlled the pumps and the discharge rate was also verified with an acoustic flowmeter.

Table 1 | Discharges tested

Label	Q0.5	Q1	Q2	Q3	Q4	Q5	Q6
Q_{in} [m^3/s]	0.005	0.010	0.020	0.030	0.040	0.050	0.060
h_{in} [m]	0.017	0.027	0.041	0.053	0.065	0.075	0.083
u_{in} [m/s]	0.58	0.75	0.97	1.12	1.24	1.34	1.42

Water depths were obtained using two different methods in four different locations (Figure 1): (1) in-house software that is based on video and photographs, allowing a visual verification of the measurements (Roque 2011) by the use of a set of three photographs for each scheme, together with a video collecting obtained water height in the gully and in the outlet channel; and with (2) water resistive probes at four points (Figure 1): before the box ($x = 1.05$ [m]), L/4 of the box ($x = 1.35$ [m]), in 3L/4 of the box ($x = 1.65$ [m]) and after the box ($x = 1.95$ [m]). The second method was used to validate the first, since the first is a non-intrusive method. The results are presented in (Martins 2011; Martins *et al*. 2012) and they showed a good agreement between the values obtained with both methods.

Open foam model

The version of interFOAM (OpenFoam 1.7.1) used in this study solves the Navier Stokes equations applied to a domain with two immiscible, incompressible and isothermal fluids, using volume of fluid (VOF) to track the free surface (Hirt & Nichols 1981). InterFOAM uses a finite volume method to discretize the domain, where variable α represents the value of the cell containing each fluid, and, $0 \leq \alpha \leq 1$. When $\alpha = 1$ the cell will be completely filled with water, if $\alpha = 0$ the cell will be completely filled with

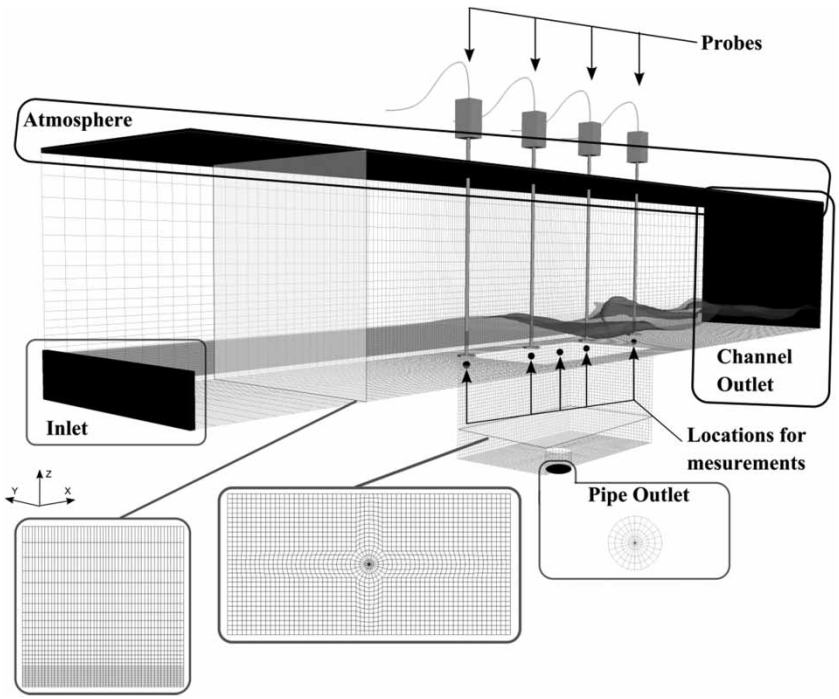

Figure 1 | 3D representation of the boundaries, probe locations, mesh details, 3D mesh, and video measurements.

air and if $0 < \alpha < 1$ there is a fraction of water and a fraction of air present in the cell. The properties v (velocity) and p (pressure) are continuous throughout the domain whereas ν (dynamic viscosity) and ρ (mass per unit volume) can contain discontinuities across the fluid separation interface (Alsgaard 2010). ρ in Equation (3) and ν in Equation (4) are

$$\rho(x, y, z, t) = \rho_{wa}\alpha + \rho_a(1 - \alpha) \tag{3}$$

$$v(x, y, z, t) = v_{wa}\alpha + v_a(1 - \alpha) \tag{4}$$

where the subscript '*wa*' refers to water, subscript '*a*' to air and *x,y,z,t* represent the spatial and temporal coordinates. The general equations of fluid flow are given by the conservation laws of physics: mass, momentum and advection equation for the volume of fluid ((5)–(7))

$$\frac{\partial \rho}{\partial t} + \nabla \cdot (\rho \mathrm{v}) = 0 \tag{5}$$

$$\frac{\partial \rho \mathrm{v}}{\partial t} + \rho a_f + \nabla \cdot (\rho \mathrm{vv}) = -\nabla p* + (\nabla \cdot (v\nabla \mathrm{v}) + (\nabla v) \cdot \nabla v) - g \cdot x\nabla\rho + k\sigma\nabla\alpha \tag{6}$$

$$\frac{\partial \alpha}{\partial t} + \nabla \cdot (\alpha \mathrm{v}) + \nabla\alpha(1 - \alpha)\mathrm{v}_{r\alpha} = 0. \tag{7}$$

With

$$\mathrm{v} = \frac{[\alpha\rho_{wa}\mathrm{v}_{wa} + (1 - \alpha)\rho_a\mathrm{v}_a]}{\rho} \tag{8}$$

$$\mathrm{v}_{vr\alpha} = \mathrm{v}_{wa} - \mathrm{v}_\alpha \tag{9}$$

Equations (6) and (7) are the momentum conservation and the volume of fluid advection as presented by Rusche (2003). In Equation (6) ρa_f is the moving reference frame term, being a_f the frame acceleration, k is the curvature of the interface air/water, σ is the surface tension, p^* is the total pressure reduced of the hydrostatic pressure and (9) is the relative velocity between air and water (Alsgaard 2010). Equation (8) represents the mass velocity.

Numerical application and assumptions

Some assumptions were made to simplify the complexity of the flow: (1) the grate was removed (either because of operational procedure or flooding conditions); (2) the outlet pipe does not surcharge (meaning the discharge in the pipe is always downwards and unobstructed); (3) the discharge entering the channel is in steady state (for each discharge tested); (4) both fluids are incompressible, isothermal and immiscible; (5) the flow in the channel is uniform, thus allowing the computational domain to be shorter (3 metres instead of the 8 metres in the experimental facility).

Table 1 defines the discharges studied. h_{in} is the uniform height of the flow and u_{in} is the velocity for a uniform discharge.

The mesh created was composed of 375,679 points and 354,500 cells. The study zone (gully) had cells with an edge of 1 cm (Figure 1) whereas the other areas had a variable edge size. The channel has a 1% slope and is 3.0 [m] long, 0.5 [m] wide and 0.5 [m] high. The gully is a parallelepiped of 0.3 [m] wide, 0.3 [m] high and 0.6 [m] long. At the bottom of the gully, a circular aperture with a 0.08 [m] diameter has a pipe of 0.05 [m] length with a free exit.

Four patches were defined: 'wall', 'inlet', 'outlet and 'atmosphere'. On the inlet, the velocity (u_{in}) was defined based on the uniform discharge (Table 1), with the height of the patch equal to h_{in}. Both outlets (pipe outlet and channel outlet) and atmosphere were defined as having a relative pressure of 0 [Pa]. The boundary areas not mentioned are defined as wall, i.e. with 0 velocity [m/s] in all directions. The initial condition is set as a constant water level in the whole domain with height equal to the top of the inlet and initial velocity (in the channel) equal to the velocity imposed at the inlet. The last 5 seconds of the simulation were averaged in all parameters. The simulations were performed for 20 seconds and steady state was achieved (Martins 2011).

RESULTS

Water depth

Comparison between experimental and numerical results is presented in Figure 2 and Table 2 for the four lowest discharges.

Table 2 shows numerical and experimental results at the three main locations inside the gully (L/4, L/2 and 3L/4 in Figure 2(b)) along with the error observed. The reference level of the bottom of the gully is 0.3 [m]. Three global coefficients are also presented for the evaluation of the fitness of data: (1) the root mean squared deviation (RMSD) shown in Equation (10), where x represents the experimental values, y the numerical values, n the total number of samples and i

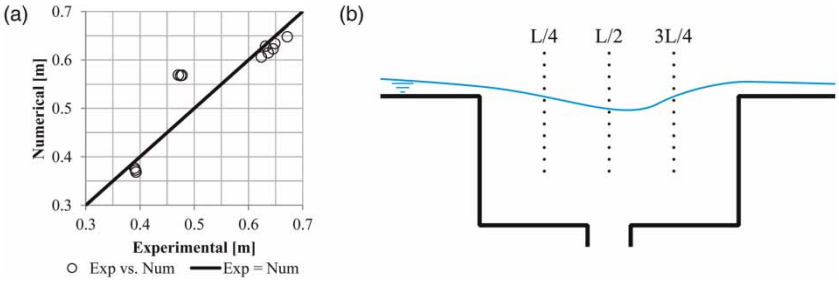

Figure 2 | Comparison between numerical and experimental values: (a) – comparison graph; (b) – comparison locations.

Table 2 | Comparison between numerical and experimental value results: errors and RMSDs

Units	Discharge [m³/s]	L/4 [m]	L/2 [m]	3L/4 [m]
Experimental	0.005	0.390	0.393	0.392
	0.01	0.471	0.475	0.478
	0.02	0.631	0.624	0.636
	0.03	0.649	0.645	0.672
Numerical	0.005	0.376	0.368	0.372
	0.01	0.569	0.568	0.568
	0.02	0.629	0.606	0.614
	0.03	0.634	0.623	0.648
Error	0.005	2.1%	5.5%	6.2%
	0.01	20.8%	19.5%	19.0%
	0.02	0.5%	2.8%	3.5%
	0.03	2.3%	3.5%	3.6%
RMSD				0.050
NRMSD				18%
CV(RMSD)				9%

the counter; (2) normalized root mean squared deviation (Equation (11)), which is obtained by dividing the RMSD by the absolute difference between the maximum and the minimum values of the observed values; (3) coefficient of variation of the RMSD (Equation (12)) where the RMSD is divided by the absolute average value of the observed values. Smaller values imply a better fit of the data

$$RMSD = \sqrt{\frac{\sum_{i=1}^{n} (x_i - y_i)^2}{n}} \quad (10)$$

$$NRMSD = \frac{RMSD}{|\max(x_i) - \min(x_i)|} \quad (11)$$

$$CV(RMS) = \frac{RMSD}{|\bar{x}|} \quad (12)$$

Figure 2(a) presents in a graph the results from the experimental and numerical analysis. Each circle represents the two heights obtained for the experimental (bottom axis) and the numerical results (left axis). The line represents the position where the experimental results equal the numerical and, therefore, better adjustment.

Pressure and velocity

To characterize the hydraulic behaviour of the gully pressure and velocity, profiles are displayed along a centred vertical plane aligned with the incoming flow from the surface channel. The vertical plane coincides with the location of the probe measurements (Figure 1). Figure 3 and 4 show the pressure and velocity profiles obtained numerically in the vertical plane of the gully together with the two side walls, bottom and outlet.

Figure 3 shows the pressure in the left and right wall. The bottom horizontal axis represents the pressure for both the left and the right wall (left-to-middle for the left wall and middle-to-right for the right wall). The dimensions of the gully are represented in the vertical axis by the overall z coordinate (0.3 [m] is the relative height of the bottom of the gully) and in the top axis by a relative x coordinate.

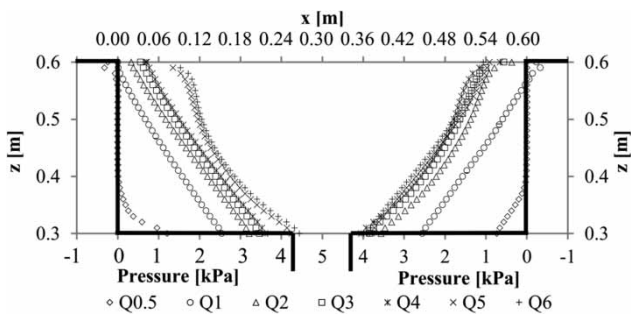

Figure 3 | Pressure values for the middle plane of the gully in the left and right walls.

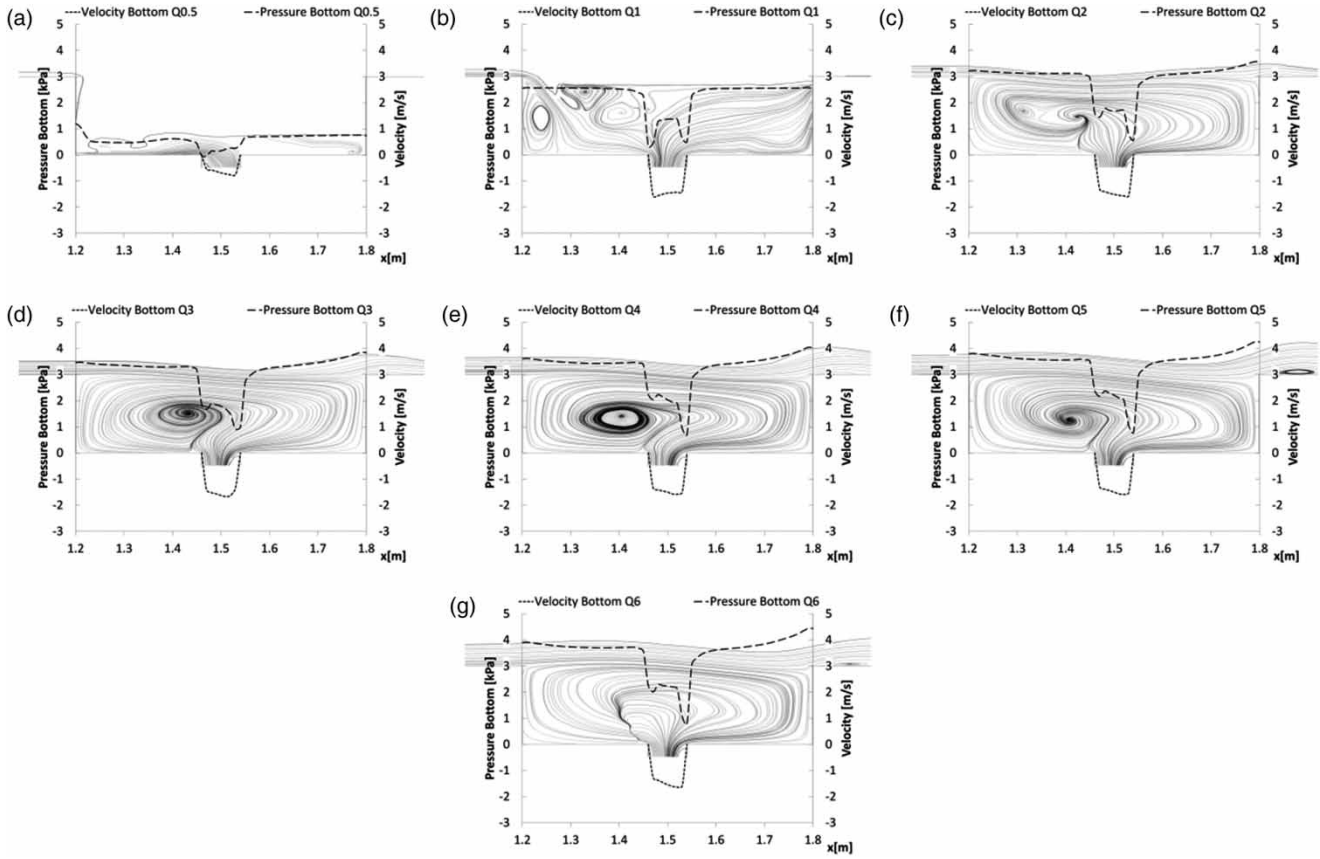

Figure 4 | Streamlines in the middle section of the gully, pressure and velocity for the bottom middle section inside the gully.

The bottom pressure, the velocity and the streamlines for the middle plane are represented in Figure 4(a)–(g). The pressure is represented in the left axis for the bottom of the gully for each discharge; the velocity is represented on the right axis for the entrance of the pipe. For the pressure and the velocity, the bottom axis represents the global x coordinate. The averaged streamlines are represented for the entire middle plane.

Discharge coefficients

Figure 5(a) shows the discharge results from the numerical and the experimental simulations. The left vertical axis represents the measured discharge experimentally and numerically, the bottom horizontal axis represents the design discharge from Table 1 (Q_{in}) and the right vertical axis shows the difference obtained between the numerical and the experimental data divided by the latter (relative error). Inlet, pipe outlet and channel outlet discharges are represented by lines (square with a dashed line for the inflow, circle with a full line for the pipe outlet, and triangle with a dotted line for the channel outlet) with full markers for the experimental data and hollow for the numerical data. Inlet height observation point is 1 metre upstream of the gully. The numerical discharges were obtained by integrating the velocity in a section 0.01 [m] away from the boundary conditions. The relative error is represented by markers in grey.

Discharge coefficients obtained numerically and experimentally can be seen in Figure 5(b) and Table 3.

In Figure 5(b), the left axis represents the discharge coefficients and the bottom axis represents the water height upstream. Power laws were fitted to the data, excluding the first point for the experimental and numerical data. The coefficients are presented in Table 4 and applied in Equation (13)

$$C = a * h_{in}^{b} \tag{13}$$

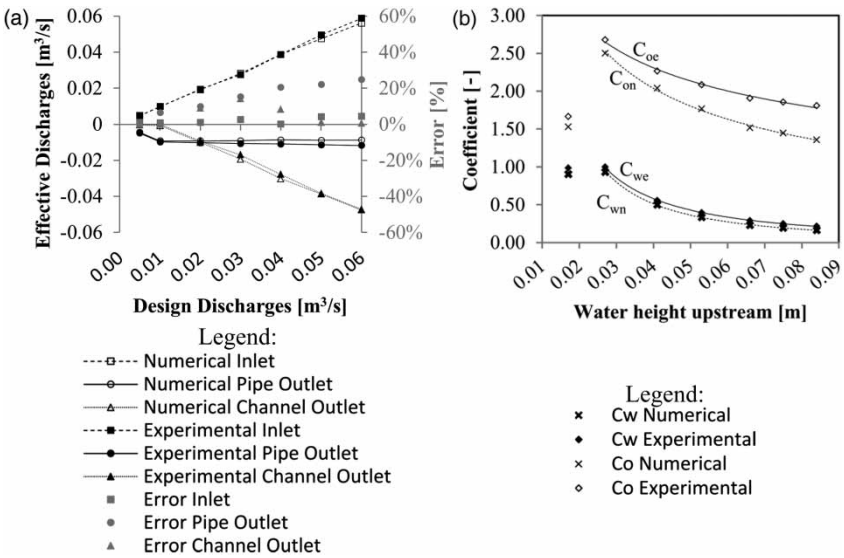

Figure 5 | (a) Comparison between experimental and numerical data; (b) discharge coefficients with a power law fit.

Table 3 | Flow coefficients table (C_w – weir; C_o – orifice)

Discharge		Q6	Q5	Q4	Q3	Q2	Q1	Q0.5
Numerical data	C_w	0.16	0.19	0.23	0.33	0.50	0.93	0.90
	C_o	1.36	1.45	1.51	1.77	2.04	2.50	1.53
Experimental data	C_w	0.22	0.25	0.29	0.4	0.56	1.00	0.99
	C_o	1.81	1.86	1.91	2.08	2.27	2.68	1.67

Table 4 | Power law fit coefficients and fitness

	Variable	C_{oe}	C_{on}	C_{we}	C_{wn}
Power law coefficients	a	0.75	0.35	0.0075	−1.35
	b	−0.35	−0.55	0.0035	−1.55
Fitness	R^2	0.99	1.00	1.00	1.00

DISCUSSION

Figure 2(c) shows a good agreement between the numerical and the experimental results. The good agreement is reinforced by the error values obtained for each tested discharge (below 7%) and by the global coefficient values, namely an RMSD of 0.05 [m], an NRMSD of 18% and a CV(RMS) of 9% . The discrepancy found in Q1 might be attributed to the air entrainment caused by the incoming jet of water from the left-hand side into the gully, which is known to cause inaccuracies between numerical simulations using VOF techniques and experimental results (Hussein *et al.* 1994).

The pressure profiles show an almost hydrostatic pressure in the left wall for discharges higher than 0.030 [m^3/s] while in the right wall, the profile is almost hydrostatic for values lower than 0.030 [m^3/s] (Figure 3). Figure 4 shows that there is an inversion of the position of the higher negative pressure over the orifice: for the lower discharges the higher negative pressure is situated on the left side of the orifice. However, when the gully exceeds the capacity, the higher negative pressure moves to the right side of the pipe. The same behaviour is observed with the vertical velocities; for small discharges the higher negative pressures are higher on the left side while for higher discharges they become higher on the right side of the pipe. The vortex changes to a central position on the gully.

In Figures 3 and 4 the pressure peak variations are associated with the observed displacement of the centre of the vortex. As the vortex increases in size, this induces a

change in the flow and reduces the outflow capacity, when compared to smaller discharges. Although this situation is expected, the size of the vortex and its position is of the utmost importance in characterizing the flow, especially at lower discharges. An increase in the vortex size implies that the velocities over the pipe become more horizontal-like, thus creating a threshold for gully capacity. This also induces the non-hydrostatic pressures seen in the walls (Figure 3).

In Figure 5(a), the results show a good agreement, in particular the good correlation values found in the derived discharge coefficient formulae. In Figure 5(b) the coefficients expressions are presented with the respective correlation (R^2) values. The minimum correlation obtained is 0.99 which shows a good adjustment between the numerical/experimental data and the power law curves.

CONCLUSIONS

To reproduce and characterize the hydraulic behaviour of a gully, a well-instrumented experimental facility and complex numerical models are required. The flow inside a gully is a very complex phenomenon, not only because of its three-dimensional features, but also because of its two-phase air-water interface. State-of-the-art dual-drainage models require simplified models of such linking structures in order to improve the accuracy of the water exchange between the surface and the underground sewer network.

Herein, a gully was simulated in 3D using the OpenFOAM™ toolbox. The flow inside the gully was characterized by a vertical plane aligned with the incoming surface flow and located at the centre of the gully box. Discharges ranging from 0.005–0.06 [m^3/s] were experimentally and numerically analysed. For the experimental and numerical data, empirical formulae between the flow coefficient and the height of the water upstream were derived with correlation values larger than 0.9. These formulae can be directly applied in dual-drainage models as internal boundary conditions, and thus contribute to improving the current practices in urban drainage modelling.

It is noteworthy that the observed inversion of the position of the higher negative pressure over the orifice, along with more horizontal-like velocities as the discharges increased. This behaviour is attributed to the movement of the existing vortex inside the gully and its magnitude; however, its mechanism is not fully understood. Future research will focus on understanding the role of the vortex in determining the flow behaviour inside the gully structure.

AKNOWLEDGEMENTS

The authors acknowledge the founding through FCT (Fundação para a Ciência e Tecnologia) and COMPETE (Programa Operacional Temático Factores de Competitividade), programmes supported by the European Community Fund (FEDER) through the projects PTDC/ECM/105446/2008 and PTDC/AAC-AMB/101197/2008. The first author acknowledges the contribution of FCT through the Doctoral Grant SFRH/BD/81869/2011. We also acknowledge the valuable contributions of José Roque during the data collection and for the visualisation software used for estimating the surface level, and of Joaquim Cordeiro in building the experimental facility.

REFERENCES

Alsgaard, J. A. 2010 Numerical Investigations of Piston Mode Resonance in a Moonpool Using OpenFOAM. MSc Thesis, Norwegian University of Science and Technology, Trondheim, Norway.

Bock, P., Li, W.-H. & Geyer, J. C. 1956 Hydraulic behavior of storm-water inlets: V. A simplified method of determining capacities of single and multiple inlets. *Sewage and Industrial Wastes* **28** (6), 774–784.

Carvalho, R., Leandro, J., Martins, R., Abreu, J. & de Lima, J. 2011 2DV numerical modelling of different flows occurring in gullies. In: *Proceedings 12th International Conference on Urban Drainage*, September 11–16, Porto Alegre, Brazil.

Chen, A. S., Hsu, M., Chen, T. & Chang, T. 2005 An integrated inundation model for highly developed urban areas. *Water Science and Technology* **51** (2), 221–229.

Chen, A. S., Djordjevic, S., Leandro, J. & Savic, D. 2007 The urban inundation model with bidirectional flow interaction between 2D overland surface and 1D sewer networks. In: *Proceedings of the Sixth International Conference on Sustainable Techniques and Strategies in Urban Water Management – NOVATECH 2007*, June 25–28, Lyon, France.

Djordjević, S., Prodanović, D. & Maksimović, Č. 1999 An approach to simulation of dual drainage. *Water Science and Technology* **39** (9), 95–103.

Djordjević, S., Prodanović, D., Ivetić, M. & Savić, D. 2005 SIPSON simulation of interaction between pipe flow and surface overland flow in networks. *Water Science and Technology* **52** (5), 275–283.

Hirt, C. W. & Nichols, B. D. 1981 Volume of fluid (VOF) method for the dynamics of free boundaries. *Journal of Computational Physics* **39**, 201–225.

Hussein, H. J., Capp, S. P. & George, W. K. 1994 Velocity measurements in a high-Reynolds-number, momentum-conserving, axisymmetric, turbulent jet. *Journal of Fluid Mechanics* **258**, 31–75.

Leandro, J., Djordjevic, S., Chen, A. & Savic, D. 2007 The use of multiple-linking-element for connecting surface and subsurface networks. In: *Proceedings 32nd congress of IAHR-Harmonizing the Demands of Art and Nature in Hydraulics*, July 1–6, Venice, Italy.

Leandro, J. 2008 Advanced Modelling of Flooding in Urban Areas Integrated 1D/1D and 1D/2D Models. PhD Thesis, University of Exeter, Exeter, United Kingdom.

Leandro, J., Djordjević, S., Chen, A., Savić, D. & Stanić, M. 2011 Calibration of a 1D/1D urban flood model using 1D/2D model results in the absence of field data. *Water Science and Technology* **64** (5), 1016–1024.

Li, W. H., Geyer, J. C. & Benton, G. S. 1951a Hydraulic behavior of storm-water inlets: I. Flow into gutter inlets in a straight gutter without depression. *Sewage and Industrial Wastes* **23** (1), 34–46.

Li, W. H., Sorteberg, K. K. & Geyer, J. C. 1951b Hydraulic behavior of storm-water inlets: II. Flow into Curb-Opening Inlets. *Sewage and Industrial Wastes* **23** (6), 722–738.

Li, W.-H., Goodell, B. C. & Geyer, J. C. 1954a Hydraulic behavior of storm-water inlets: III. flow into deflector inlets. *Sewage and Industrial Wastes* **26** (7), 836–842.

Li, W.-H., Goodell, B. C. & Geyer, J. C. 1954b Hydraulic behavior of storm-water inlets: IV. Flow into depressed combination inlets. *Sewage and Industrial Wastes* **26** (8), 967–975.

Martins, R., Leandro, J. & Carvalho, R. 2010 'Discharge capacity of circular orifices arranged at a flume bottom' in 'Hydraulic structures: useful water harvesting systems or relics?' In: *Proceedings of the Third International Junior Researcher and Engineer Workshop on Hydraulic Structures (IJREWHS'10)*, 2–3 May 2010, Edinburgh, Scotland (R. Jansen & H. Chanson, eds). Hydraulic Model Report CH80/10, School of Civil Engineering. The University of Queensland, Brisbane, Australia, pp. 85–92.

Martins, R. 2011 Estudo do comportamento hidráulico de sumidouros em modelo numérico OpenFOAM (Study of the Hydraulic Behaviour of Gullies in Numerical Model OpenFOAM). MSc Thesis, University of Coimbra, Coimbra, Portugal.

Martins, R., Leandro, J. & Carvalho, R. F. D. 2012 Hydraulic behaviour of a gully under drainage conditions: numerical vs. experimental. In: *Proceedings of the Ninth International Conference on Urban Drainage Modelling*, September 4–6, 2012, Belgrade, Serbia.

Nasello, C. & Tucciarelli, T. 2005 Dual multilevel urban drainage model. *Journal of Hydraulic Engineering* **131** (9), 748–754.

Roque, J. M. 2011 Medição de alturas de água usando visão computacional num modelo de Simulink (Water Measurements Using Computational Vision in a Simulink Model). MSc Thesis, University of Coimbra, Coimbra.

Rusche, H. 2003 *Computational Fluid Dynamics of Dispersed Two-phase Flows at High Phase Fractions*. Imperial College London (University of London), London, United Kingdom.

Santos, F., Carvalho, R. & Sancho, F. 2008 Performance of a multipurpose hydraulic channel. In *Proceedings of the 2nd International Junior Researcher and Engineer Workshop on Hydraulic Structures*, July–1 August 31, Pisa, Italy.

First received 11 December 2013; accepted in revised form 17 March 2014. Available online 31 March 2014